GA–A25578

PHYSICS ADVANCES IN THE ITER HYBRID SCENARIO ON DIII-D

by

P.A. POLITZER, C.C. PETTY, R.J. JAYAKUMAR, T.C. LUCE, M.R. WADE, M.A. AUSTIN, D.P. BRENNAN, T.A. CASPER, M.S. CHU, J.C. DeBOO, E.J. DOYLE, M.E. FENSTERMACHER, J.R. FERRON, P. GOHIL, C.M. GREENFIELD, C.T. HOLCOMB, A.W. HYATT, R.J. LA HAYE, C. KIM, G.R. McKEE, M.A. MAKOWSKI, M. MURAKAMI, T.W. PETRIE, R. PRATER, T.L. RHODES, G. WANG, and A.S. WELANDER

OCTOBER 2006

GENERAL ATOMICS

DISCLAIMER

GA–A25578

PHYSICS ADVANCES IN THE ITER HYBRID SCENARIO ON DIII-D

by
P.A. POLITZER, C.C. PETTY, R.J. JAYAKUMAR,* T.C. LUCE, M.R. WADE, M.A. AUSTIN,[†] D.P. BRENNAN,[‡] T.A. CASPER,* M.S. CHU, J.C. DeBOO, E.J. DOYLE,[¶] M.E. FENSTERMACHER,* J.R. FERRON, P. GOHIL, C.M. GREENFIELD, C.T. HOLCOMB,* A.W. HYATT, R.J. LA HAYE, C. KIM,[§] G.R. McKEE,[§] M.A. MAKOWSKI,* M. MURAKAMI,[#] T.W. PETRIE, R. PRATER, T.L. RHODES,[¶] G. WANG,[¶] and A.S. WELANDER

This is a preprint of a paper to be presented at the 21st IAEA Fusion Energy Conference, October 16-21, 2006, in Chengdu, China, and to be published in the *Proceedings.*

*Lawrence Livermore National Laboratory, Livermore, California.
[†]University of Texas-Austin, Austin, Texas.
[‡]University of Tulsa, Tulsa, Oklahoma.
[¶]University of California-Los Angeles, Los Angeles, California.
[§]University of Wisconsin-Madison, Madison, Wisconsin.
[#]Oak Ridge National Laboratory, Oak Ridge, Tennessee.

Work supported by
the U.S. Department of Energy
under DE-FC02-04ER54698, W-7405-ENG-48, DE-FG03-97ER54415, DE-FG03-01ER54615, DE-FG03-96ER54373, and DE-AC05-00OR22725

GENERAL ATOMICS PROJECT 30200
OCTOBER 2006

Physics Advances in the ITER Hybrid Scenario on DIII-D

P.A. Politzer 1), C.C. Petty 1), R.J. Jayakumar 2), T.C. Luce 1), M.R. Wade 1),
M.E. Austin 3), D.P. Brennan 4), T.A. Casper 2), M.S. Chu 1), J.C. DeBoo 1), E.J. Doyle 5),
M.E. Fenstermacher 2), J.R. Ferron 1), P. Gohil 1), C.M. Greenfield 1), C.T. Holcomb 2),
A.W. Hyatt 1), R.J. La Haye 1), C. Kim 6), G.R. McKee 6), M.A. Makowski 2),
M. Murakami 7), T.W. Petrie 1), R. Prater 1), T.L. Rhodes 5), G. Wang 5),
and A.S. Welander 1)

1) General Atomics, P.O. Box 85608, San Diego, California 921860-5608, USA
2) Lawrence Livermore National Laboratory, Livermore, California, USA
3) University of Texas-Austin, Austin, Texas, USA
4) University of Tulsa, Tulsa, Oklahoma, USA
5) University of California-Los Angeles, Los Angeles, California, USA
6) University of Wisconsin-Madison, Madison, Wisconsin, USA
7) Oak Ridge National Laboratory, Oak Ridge, Tennessee, USA

e-mail contact of main author: politzer@fusion.gat.com

Abstract. We report significant progress in our understanding of hybrid plasmas on DIII-D, particularly for ITER-relevant low rotation. With the new counter-neutral beam injection (NBI) capability, the central Mach number has been reduced by up to a factor of 6 compared to co-NBI discharges. Although energy confinement decreases and the 3/2 NTM amplitude increases for low Mach number, $\beta_N H_{89P}/q_{95}^2$ still exceeds the value required on ITER for $Q_{fus} = 10$. Hybrid plasmas with a dominant 4/3 NTM have reduced transport compared to 3/2 NTM hybrids, with χ_i approaching χ_{neo}. Energy loss is dominated by χ_e, consistent with nonlinear GYRO simulations. Ongoing experiments are attempting to determine the physical mechanism that reduces or eliminates sawteeth in hybrid plasmas. Detailed analysis of the motional Stark effect signals indicates that coupling between the edge localized modes and 3/2 NTM broadens the current density profile, but the role of kinetic Alfvén wave and energetic particle redistribution is still being investigated and has not been ruled out. These observations provide optimism about the projections of the hybrid scenario to low rotation plasmas in ITER, but they also indicate the need for a better understanding of the physics of toroidal rotation.

1. Introduction

Experiments on the DIII-D tokamak have developed a long duration, high performance plasma discharge that is an attractive operating scenario for ITER [1,2]. Distinct from both the standard H-mode scenario and the Advanced Tokamak regime, this hybrid scenario regime is inductively driven, with bootstrap current fraction of 0.3-0.5 and a fully relaxed current profile with $q_0 \sim 1$. Compared to standard H-mode operation, the hybrid plasma has a broader current profile that is less susceptible to the onset of $m/n = 2/1$ neoclassical tearing modes (NTMs), allowing higher β operation. The broad current profile also yields lower calculated growth rates for drift wave turbulence, allowing higher confinement. In addition, the broader current profile in the hybrid regime often eliminates sawteeth, further improving overall confinement and removing a trigger for the 2/1 NTM [3]. At $q_{95} \approx 3.2$, the fusion performance parameter $G(= \beta_N H_{89P}/q_{95}^2)$ has been maintained at $G = 0.7$ with stationary conditions for over five current relaxation times, well above the value of $G = 0.42$ projected for ITER operation at $Q_{fus} = 10$.

In recent DIII-D experiments we have studied the MHD and transport properties of the hybrid scenario plasma, as well as the changes in characteristics and performance of the hybrid plasma as the toroidal rotation velocity is reduced. There is a stationary level of MHD activity

in all hybrid scenario plasmas in DIII-D. This most often is an $m/n = 3/2$ NTM, although occasionally a 4/3 NTM or fishbone modes are seen. The 3/2 NTM has the beneficial effect in hybrid plasmas of broadening the current profile and maintaining $q_0 > 1$ without sawteeth for $q_{95} > 4$ (with very small sawteeth for $q_{95} \leq 4$). Transport in hybrid plasmas is dominated by electron heat conduction, but the observed electron thermal diffusivity is relatively small. The ion thermal diffusivity is consistently at or close to the neoclassical value. Using the recent modification to the DIII-D neutral beam configuration, we have been able to reduce the toroidal rotation velocity by up to a factor of 6, to $M \approx 0.075$ (M = Mach number = v_ϕ/v_s), under stationary conditions. Under conditions of low rotation, confinement is reduced and the width of the NTM island increases. However, the reduction in G is only 10%-30%.

2. Rotation

Recent hybrid experiments have used the newly installed counter-injection neutral beam capability on DIII-D to survey the dependence of hybrid performance on rotation. These discharges were operated with a fixed level of counter-NBI power, using the plasma control system to adjust the co-NBI power to maintain an approximately constant level of β_N (within $\delta\beta_N \approx \pm 0.05$; typically in the range $\beta_N = 2.5$-2.9). The principal observation is that the Mach number M can be significantly reduced with only a modest reduction in G. For high q_{95} (≥ 3.8) M is observed to be as low as 0.075 with an 18% reduction in G. Perhaps of more direct relevance to ITER scenarios, at low q_{95} (~3.3) a hybrid plasma has been maintained under stationary conditions for >4.5 s at $M = 0.10$, with $\beta_N = 2.7$ and $G = 0.47$.

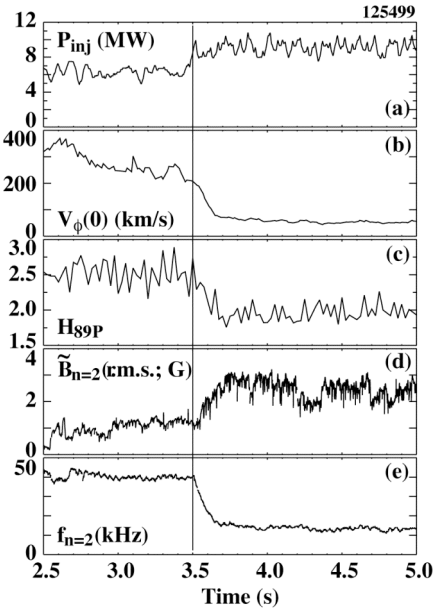

FIG. 1. Time dependence of key parameters when the NBI torque is reduced; (a) injected NBI power, (b) toroidal velocity near the magnetic axis, (c) H_{89P} confinement parameter, (d) $n = 2$ NTM fluctuation amplitude, and (e) NTM frequency. The counter beams are turned on at 3.5 s. A new stationary state is established after about 250 ms.

An example of a low rotation, high q_{95} stationary case (125499) is shown in Fig. 1. Here, the initial power and torque are 6.4 MW and 4.9 N-m, respectively (not corrected for shine-through or first orbit losses). At 3.5 s, the power rises to 9.4 MW (co: 5.2, ctr: 4.2) and the torque drops to 1.0 N-m (co: 4.2, ctr: –3.2). The toroidal velocity at the magnetic axis decreases by a factor of ~4.2, the $n = 2$ rms magnetic field amplitude at the Mirnov probes increases by ~4.0, the $n = 2$ mode frequency decreases by ~3.1, and H_{89P} (not corrected for shine-through or first orbit losses) decreases by ~1.3, as does the parameter G.

Figure 2 shows the profiles for discharge 125499 with co-NBI only (averaged 2.99-3.48 s) and with nearly balanced beams (averaged 4.02-5.72 s). There is little change in the shapes of the kinetic profiles; the temperatures are somewhat lower and the density is somewhat higher. The toroidal rotation of the carbon ions is reduced uniformly, except that it becomes negative near the edge. The changes in the current and q profiles are small. The current profile broadens somewhat ($\delta\ell_i \approx -0.04$) due to changes in the outer half of the plasma, but the location of the $q = 1.5$ surface does not change. Figure 3 shows the changes in the profiles of the NBI torque and current drive, before and after the counter beams are turned on. Both the

torque profile and the neutral beam current drive (NBCD) profile are strongly affected. The torque is reduced by a factor of ~3 at $\rho = 0.2$ and a factor of ~2 at $\rho = 0.5$, becoming strongly negative for $\rho > 0.8$. In contrast the NBCD profile is broadened, being reduced by a factor of ~4 at $\rho = 0.2$ and ~2 at $r = 0.5$, with much less reduction at larger radii. Figure 4 shows the changes in χ_i, χ_e, and χ_Ω when the rotation is reduced. The transport coefficients inferred by TRANSP analysis increase by a factor of 1.5-2 in the plasma core when the torque is reduced by roughly a factor of 4 (Fig. 3). The change in the radial shearing rate of the ExB flow is large for $0.4 \le \rho \le 0.85$ (Fig. 5). Near the axis the shearing rate is small regardless of the rotation.

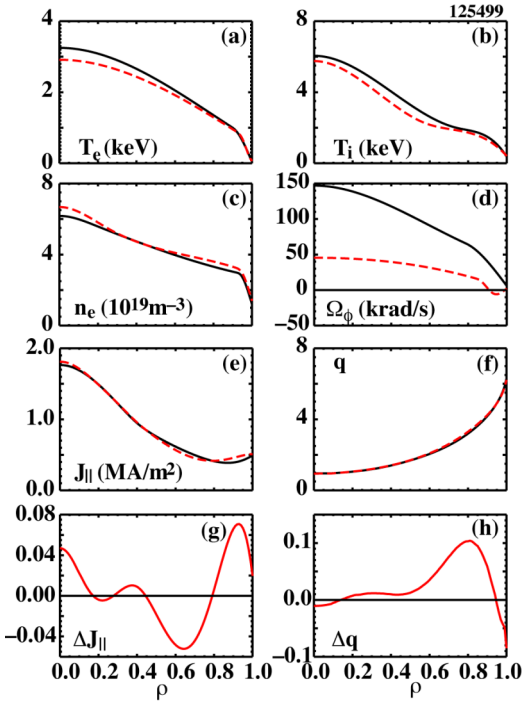

FIG. 2. Changes in profiles without and with counter-NBI. Solid black lines are averages over 2.99-3.48 s; dashed red lines are for 4.05-5.72 s (also in Figs. 3-5). (a) T_e, (b) T_i, (c) n_e, (d) Ω_ϕ, (e) $\langle J_{||} \rangle$, (f) q, (g) $\Delta\langle J_{||} \rangle$, and (h) Δq.

We find that, below a critical rotation level a stationary state cannot be maintained for an extended period. Instead the braking due to the residual static error field and to the interaction between the 3/2 NTM and the wall causes the rotation to continue to decrease. Then either the 3/2 mode locks to the wall or an $m/n = 2/1$ mode is destabilized and soon locks. In either case, even though the rotation goes to a small negative value, a locked $n = 1$ perturbation appears and there is a significant loss in confinement (but not a disruption). Presumably the rotation at which this mode locking process begins depends on the quality of the error field correction being applied, although no specific tests of this have been done. We find that the maximum negative torque for which a stationary, low rotation condition can be maintained increases with density and with q_{95}; i.e., it is easier to cause locking at low density and at low q_{95}. Future experiments using feedback control of the toroidal rotation will try to avoid this locking phenomenon by adjusting the amount of NBI torque.

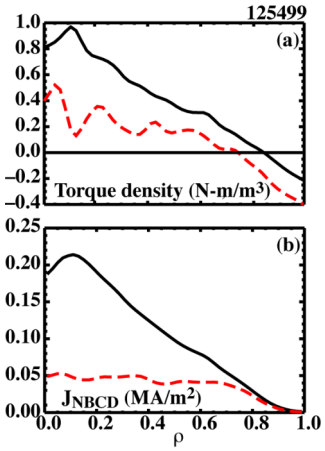

FIG. 3. Changes in the profiles of NBI torque density and NBCD.

We have developed a database of 417 DIII-D hybrid scenario discharges (2000-06) which have stationary conditions for at least 1 s (and up to 8 s). The database contains global (scalar) parameters averaged over the stationary interval for each discharge. The dependence of gross confinement on rotation rate is shown in Fig. 6, a scatterplot showing H_{89P} (uncorrected for beam shine-through or first orbit losses) versus the central Mach number. All points with $M_0 \le 0.2$ are from the recent counter-injection experiments. H_{89P} has a weak dependence on $M_0 (\delta H_{89P}/\delta M_0 \approx 0.18)$, but there is no sharp break that would indicate a change in the underlying physical processes causing transport.

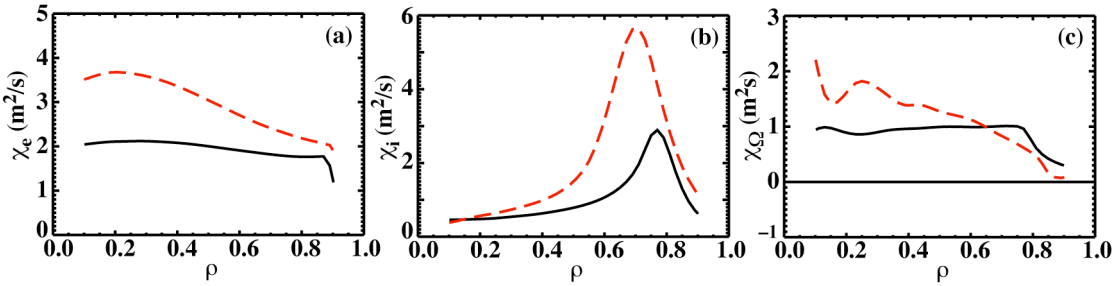

FIG. 4. Changes in the profiles of (a) electron, (b) ion, and (c) toroidal angular momentum diffusivities from TRANSP analysis.

3. Transport

Hybrid plasmas exhibit excellent overall confinement. The mean value of $\langle H_{89} \rangle$ in our hybrid database is 2.36 (including the low rotation plasmas; the $\langle\rangle$ indicate averaging over the stationary phase of the discharge), with 30% of the discharges exceeding $\langle H_{89} \rangle = 2.5$. There is a weak dependence of $\langle H_{89} \rangle$ on density, decreasing by about 15% for a doubling of the line-averaged density from 3.5×10^{19} m^{-3} to 7×10^{19} m^{-3}. There is no statistically significant dependence of $\langle H_{89} \rangle$ on q_{95}.

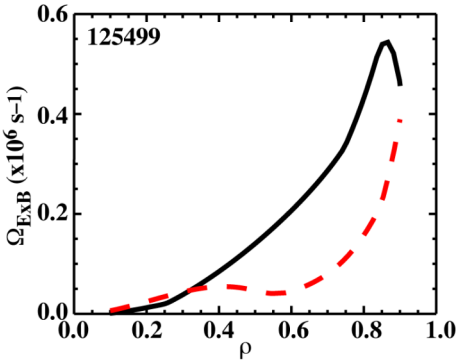

FIG. 5. Change in the profile of the shearing rate of the ExB flow.

Detailed transport analysis of individual discharges shows that the electron and ion thermal diffusivities, χ_e and χ_i, are relatively small but that the electron channel consistently dominates the conduction loss. Figure 7 compares χ_e and χ_i for hybrid discharges with a 3/2 NTM and with a 4/3 NTM. Both discharges have $q_{95} = 3.1$. The 3/2 NTM dominated discharge has $\beta_N = 2.6$, and $H_{89P} = 2.3$; the 4/3 NTM dominated discharge has $\beta_N = 2.65$ and $H_{89P} = 2.6$. While even for the 3/2 NTM case χ_i is only twice the neoclassical level around $\rho \approx 0.5$, χ_e is more than four times χ_i at the same location for both cases. The domination of the energy loss by electron heat conduction is consistent with nonlinear GYRO [4] simulations showing that the ETG mode and the TEM cause the majority of transport, although these modes are predicted to be linearly stable

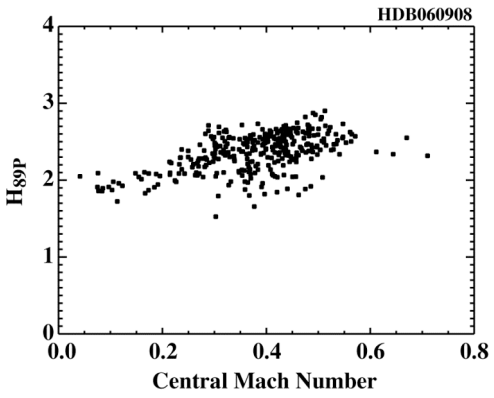

FIG. 6. H_{89P} vs central Mach number from a database of hybrid discharges which are stationary for >1 s.

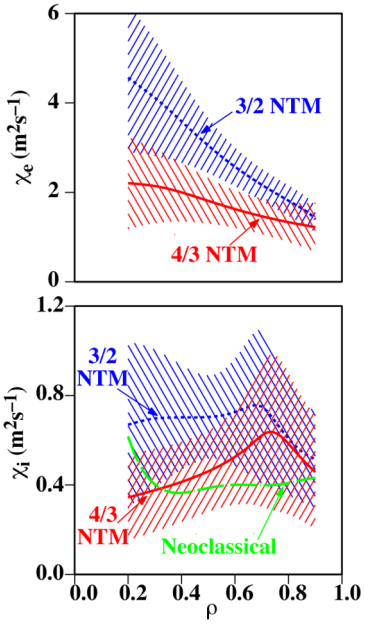

FIG. 7. Comparison of electron and ion thermal diffusivities for a 4/3 NTM dominated (red; solid) and a 3/2 NTM dominated (blue; dashed) plasma. Also shown is χ_{ineo} (green; dash-dot).

in the core. While a low level of ion heat conduction is also consistent with transport simulations, the experimental χ_i profile is not entirely understood as the GKS gyrokinetic stability code predicts that the ITG mode should be weakly unstable in the outer half of the plasma (for $\rho \geq 0.5$-0.6) and stable in the inner half. For the higher q_{95} cases, the value of χ_i inferred from measurements increases somewhat, especially in the outer part of the plasma, but electron heat transport still dominates.

Depending on initial conditions, hybrid scenario discharges on DIII-D can have a dominant 4/3 NTM instead of a dominant 3/2 NTM. The 4/3 NTM dominated discharges typically have 15% higher values of H_{89P} than the 3/2 NTM discharges. One explanation for the difference is the flattening of the pressure profile in the vicinity of the $q = 1.5$ surface, as seen in Fig. 8. Here we plot the results of an analysis of the motional Stark effect (MSE) diagnostic data, which yields pressure, bootstrap current, Pfirsch-Schlüter current, and other equilibrium profiles directly, without equilibrium reconstruction [5]. The "missing" bootstrap current due to the flattening of the pressure profile by the 3/2 island is clearly seen here for the first time. The reduction due to the 4/3 island is much smaller. A second reason for the improved confinement in the 4/3 NTM plasmas is higher ExB velocity. Figure 9 shows that, compared to a 3/2 NTM hybrid plasma, the 4/3 NTM plasma has a higher toroidal rotation rate in the core owing to smaller island drag effects. The 4/3 NTM hybrid plasma shown in Fig. 7 (solid red curves) was sustained for ~5 current relaxation times with $G = 0.7$, which is 70% above the value projected for $Q_{fus} = 10$ operation in ITER. χ_e is systematically lower for the 4/3 NTM hybrid case in Fig. 7 compared to the 3/2 NTM hybrid case, which mostly accounts for the improved confinement factor. The measured χ_i profile for the 4/3 hybrid case is remarkably close to the neoclassical value across the entire plasma. While several realizations of the hybrid scenario have been reported on other tokamaks [6-8], the dominant 4/3 NTM scenario appears to be unique to DIII-D.

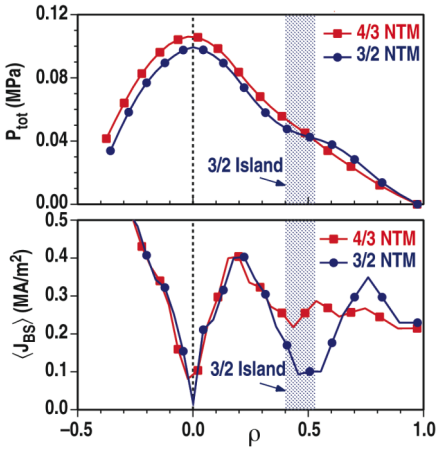

FIG. 8. Direct analysis of motional Stark effect signals without equilibrium reconstruction for hybrid discharges with a dominant 4/3 NTM (red) or 3/2 NTM (blue) showing (a) total pressure profile, and (b) bootstrap current density profile.

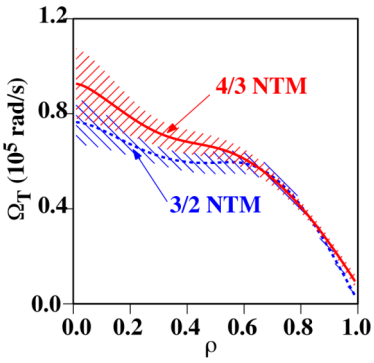

FIG. 9. Comparison of the toroidal rotation profiles for a 4/3 NTM hybrid (red; solid) and a 3/2 NTM hybrid (blue; dashed).

Other transport studies on DIII-D have measured for the first time the ρ* scaling of heat transport in hybrid plasmas, with the other dimensionless parameters kept constant. For discharges with $q_{95} > 4$, a scan of ρ* by a factor of 1.6 has indicated that the effective diffusivity has a scaling close to gyroBohm-like in the core, but becoming more Bohm-like near the edge. We have also done experiments applying 3rd harmonic electron cyclotron heating to hybrid plasmas with $T_i > T_e$ and have measured a decrease in toroidal rotation and an increase in χ_e and χ_i. This result is similar to

observations in standard H-mode plasmas with $T_i > T_e$, where the electron heating is predicted to have a destabilizing effect on the ITG mode.

As reported in another paper at this conference [9], a radiative divertor has been successfully applied to the hybrid scenario using argon injection, with good core confinement and high levels of radiation ($P_{rad}/P_{input} = 0.6$) simultaneously achieved. High impurity enrichment ($\eta_{Ar} > 30$) in the divertor has been demonstrated. Another paper at this conference [10] describes the stabilization of the $m/n = 2/1$ NTM in hybrid plasmas using ECCD and the avoidance of the 2/1 mode entirely with preemptive ECCD, enabling an increase of β_N to the no-wall limit.

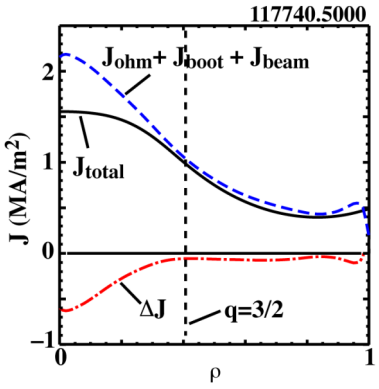

FIG. 10. Total parallel current from equilibrium reconstruction (with MSE data) of discharge 117740 at 5000 ms (black; solid); sum of the Ohmic, bootstrap, and NBCD currents (blue; dashed); difference between these (red; dash-dot).

4. MHD and Current Profile

MHD activity in tokamak plasmas is usually deleterious. However, in the hybrid scenario the presence of stationary MHD activity modifies the current profile so as to improve both confinement and the operational β limit. The gain in overall performance outweighs the cost in confinement due to the presence of an island structure. In the presence of the 3/2 NTM, the central current density is reduced relative to predictions using neoclassical resistivity, raising the central value of the safety factor, q_0 (Fig. 10). While the current density at the magnetic axis can be reduced by as much as a third, relative to the neoclassical case, the integral of the redistributed current is only 5%-10% of the total current.

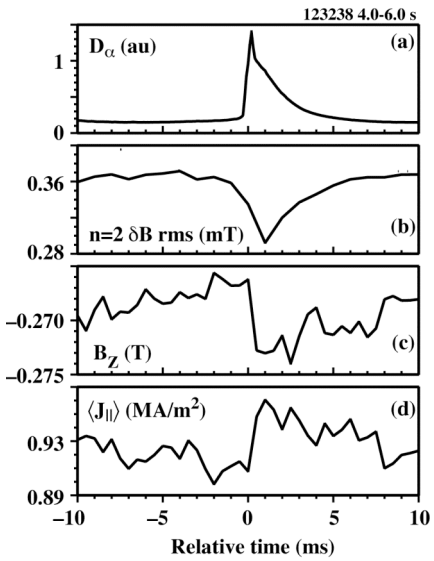

FIG. 11. Time histories of key parameters at an ELM, averaged over 112 ELMS. (a) D_α signal at the divertor target; (b) NTM amplitude; (c) poloidal (vertical) magnetic field at the outboard midplane location of the q = 3/2 surface; and (d) parallel current density at the same location as (c).

The connection between the 3/2 NTM and the redistribution of current has been established by modifying the NTM amplitude using ECCD. Co-ECCD stabilizes the mode, resulting in lower q_0 and larger sawteeth. On the other hand, counter-ECCD leads to increased mode amplitude, an increase in q_0, and smaller sawteeth [3]. Several possible mechanisms for the interaction between the NTM and the current profile have been identified. The first is based on the observed modulation of the 3/2 NTM amplitude by edge localized modes (ELMs) [11]. This can lead to a poloidal magnetic flux pumping effect, similar to the process whereby sawteeth maintain $q_0 \approx 1$. Looking at the average change in poloidal field and parallel current at the $q = 1.5$ surface for a sequence of ELMs during the stationary phase of a discharge (Fig. 11) shows a fast rearrangement of the current density profile during the ELM. Figure 12 shows the change in the profiles of B_Z, q, $J_{||}$, and J_{bs} when an ELM occurs. The changes at the $q = 1.5$ surface indicate the effect of the ELM modulation of the 3/2 island width is to increase q inside the $q = 1.5$ surface.

A second possible mechanism for current redistribution near the magnetic axis is associated with the presence of an $m/n = 2/2$ component of the global 3/2 NTM. A model study of the radial structure of the $n = 2$ NTM (Fig. 13) shows that the relative amplitude of the $m/n = 2/2$ component is very sensitive to $q_0 - 1$, becoming large as $q_0 - 1 \to 0$. In the plasma frame at the axis, this component appears as a traveling wave because it is co-rotating with the island at the $q = 1.5$ surface, and because of the rotation shear between the $q = 1.5$ surface and the axis. The possibility of mode conversion of this perturbation to a kinetic Alfvén wave (KAW), and the physics of current drive by the KAW are discussed in another paper at this conference [12].

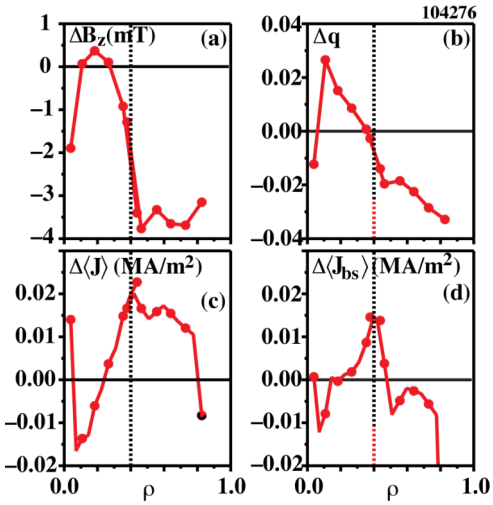

FIG. 12. Differences between the profiles after the ELM and before the ELM in the (a) poloidal magnetic field at the outboard midplane, (b) the safety factor, (c) the average parallel current density, and (d) the bootstrap current. The vertical dashed line indicates the location of the q = 3/2 surface.

It is also possible that there is a radial redistribution of the beam-injected fast ions, either by the NTM itself, by the KAW discussed above, or by the ELM modulation of the NTM, resulting in broadening of the NBCD profile. Although there are no large changes in the confinement of fast ions, evidenced by the observation that the neutron flux does not change when the 3/2 NTM appears or changes amplitude, even a small redistribution of the ions would be sufficient to produce the observed change in q_0. Note that the estimated current redistribution by the NTM needs to be about 25% of the total NBCD (typically 50 kA versus 200 kA) (Fig. 10).

The spatial structure of the NTM has been examined both in the density variation, with the beam emission spectroscopy (BES) diagnostic, and in the electron temperature variation, with the electron cyclotron emission (ECE) diagnostic (Figs 14 and 15). For this discharge, both measurements indicate a 5-8 cm wide island at the $q = 1.5$ surface on the outboard midplane. The T_e perturbation does not vanish near the magnetic axis, but is about 30% of the maximum perturbation near the NTM island. There is a phase shift of $\sim 2\pi/3$ between the perturbations at the island and at the axis, which may be indicative of the presence of the 2/2 component.

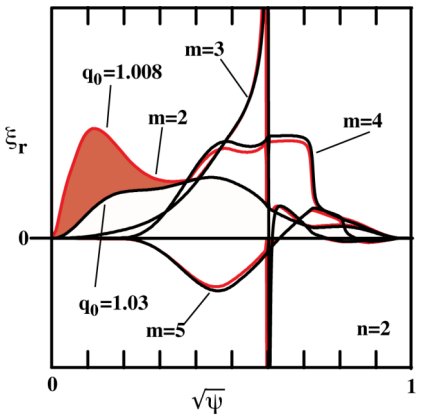

FIG. 13. m = 2, 3, 4, 5 displacements of n=2 mode versus $q(0)$ from PEST3.

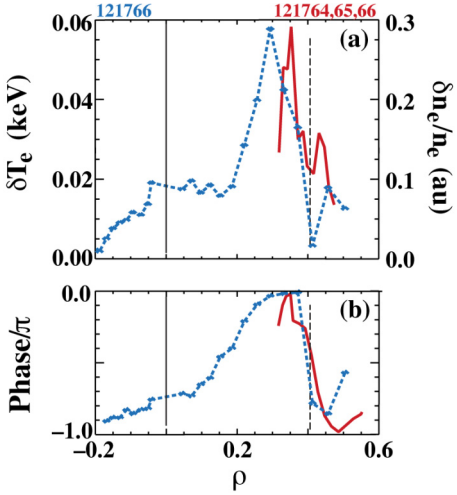

FIG. 14. 3/2 amplitude and phase on ECE (blue) and BES (red).

5. Summary

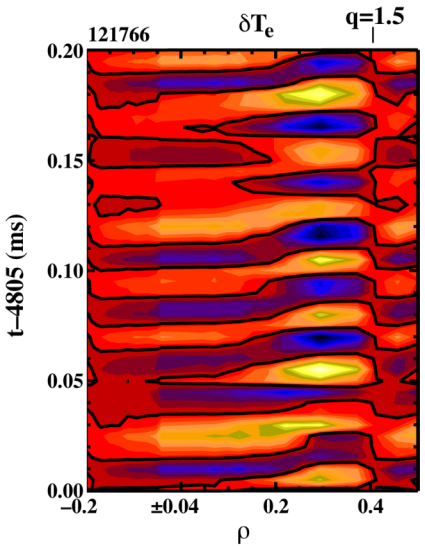

FIG. 15. Contour plot of temperature perturbation vs time and radius.

Significant progress has been made in our understanding of the properties of hybrid plasmas on DIII-D, especially in regard to ITER-relevant low rotation scenarios. Using the newly installed counter beam injection capability of DIII-D, the central Mach number has been reduced by a factor of 6 compared to co-NBI discharges. While the energy confinement time decreases (likely owing to ExB shear reduction) and the 3/2 NTM amplitude increases for low rotation conditions, the fusion performance factor still exceeds the value required on ITER for $Q_{\mathrm{fus}} = 10$ operation. The rotation experiments have provided some unification of our understanding of hybrid plasmas since the effects of counter-NBI, error fields, and external magnetic perturbations appear to be the same when sorted by the achieved Mach number. Hybrid plasmas with a dominant 4/3 NTM have reduced transport compared to 3/2 NTM hybrids, due to a less significant island and a faster core rotation rate, with the ion thermal diffusivity approaching the neoclassical value. Electron heat conduction clearly dominates the energy loss process, which is consistent with nonlinear GYRO simulations that show the ETG mode and TEM cause the majority of transport. Ongoing experiments are attempting to determine the physical mechanism that reduces or eliminates sawteeth in hybrid plasmas. Detailed analysis of the MSE signals indicates that coupling between the ELMs and 3/2 NTM broadens the current density profile (in a process similar to the effect of sawtooth oscillations), but the roles of KAW and energetic particle redistribution are still being investigated and have not been ruled out. While these observations provide optimism about the projections of the hybrid scenario to low rotation plasmas in ITER, they also point to the need for a better understanding of toroidal angular momentum transport

This work was supported by the U.S. Department of Energy under DE-FC02-04ER54698, W-7405-ENG-48, DE-FG03-97ER54415, DE-FG03-01ER54615, DE-FG02-89ER53296, and DE-AC05-00OR22725.

References

[1] LUCE, T.C., *et al.*, Nucl. Fusion **43** (2003) 321.
[2] WADE, M.R., *et al.*, Nucl. Fusion **45** (2005) 407.
[3] POLITZER, P.A., *et al.*, Proc. 32nd EPS Conf. on Plasma Physics, ECA Vol **29C** (2005) O-1.001.
[4] KINSEY, J.E., Nucl. Fusion **45** (2005) 450.
[5] PETTY, C.C., *et al.*, Plasma Phys. Control. Fusion **47** (2005) 1077.
[6] SIPS, A.C.C., *et al.*, Plasma Phys. Control. Fusion **44** (2002) A151.
[7] JOFFRIN, E., *et al.*, Plasma Phys. Control. Fusion **45** (2003) A367.
[8] ISAYAMA, A., *et al.*, Nucl. Fusion **43** (2003) 1272.
[9] PETRIE, T.W., *et al.*, this conference.
[10] PRATER, R., *et al.*, this conference.
[11] LUCE, T.C., *et al.*, Phys. Plasmas **11** (2004) 2627.
[12] CHU, M.S., *et al.*, this conference.